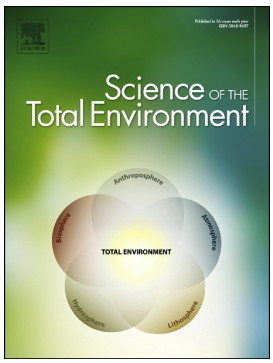

Fixed-bed performance of a waste-derived granular activated carbon for the removal of micropollutants from municipal wastewater

Guilaine Jaria, Vânia Calisto, Carla Patrícia Silva, María Victoria Gil, Marta Otero, Valdemar I. Esteves

PII: S0048-9697(19)32237-5
DOI: https://doi.org/10.1016/j.scitotenv.2019.05.198
Reference: STOTEN 32359

To appear in: *Science of the Total Environment*

Received date: 12 February 2019
Revised date: 14 May 2019
Accepted date: 14 May 2019

Please cite this article as: G. Jaria, V. Calisto, C.P. Silva, et al., Fixed-bed performance of a waste-derived granular activated carbon for the removal of micropollutants from municipal wastewater, Science of the Total Environment, https://doi.org/10.1016/j.scitotenv.2019.05.198

Fixed-bed performance of a waste-derived granular activated carbon for the removal of micropollutants from municipal wastewater

Guilaine Jaria[1], Vânia Calisto[1*], Carla Patrícia Silva[1], María Victoria Gil[2], Marta Otero[3], Valdemar I. Esteves[1]

[1]*Department of Chemistry & CESAM, University of Aveiro, Campus de Santiago, 3810-193 Aveiro, Portugal*

[2]*Instituto Nacional del Carbón, INCAR-CSIC, Calle Francisco Pintado Fe 26, 33011 Oviedo, Spain*

[3]*Department of Environment and Planning & CESAM, University of Aveiro, Campus de Santiago, 3810-193 Aveiro, Portugal*

[*]corresponding author: vania.calisto@ua.pt

Abstract

This work aimed to assess the fixed-bed adsorptive performance of a primary paper mill sludge-based granular activated carbon (PSA-PA) for the removal of pharmaceuticals, namely carbamazepine (CBZ), sulfamethoxazole (SMX) and paroxetine (PAR), from water. The breakthrough curves corresponding to the adsorption of CBZ at different flow rates and in two different matrices (distilled and urban wastewater) were firstly determined, which allowed to select the most favorable flow rate for the subsequent experiments. The fixed-bed adsorption of CBZ, SMX and PAR from single and ternary solutions in wastewater showed that the performance of PSA-PA was different for each pharmaceutical. According to the obtained breakthrough curves, the poorest bed adsorption capacity, either from single or ternary solution, was that for SMX, which may be related with electrostatic repulsion at the pH of the wastewater used (pH ~ 7.3-7.7). Also, the bed adsorption capacity of PSA-PA for SMX was notoriously lower in the ternary than in the single solution, while it slightly decreased for CBZ and even increased for PAR. The regeneration studies showed that the CBZ adsorption capacity of the PSA-PA bed decreased about 38 and 71% after the first and the second thermal regeneration stages, respectively. This decline was comparatively larger than the corresponding reduction of the PSA-PA specific surface area (S_{BET}), which decreased only 5 and 25% for the first and second regeneration, respectively, and pointed to the lack of viability of more than one regeneration stage.

Keywords

Column reactor, pharmaceuticals, multicomponent adsorption, breakthrough curve, thermal regeneration

1. Introduction

The development of sustainable advanced processes is required for wastewater treatment to achieve environmental quality standards (EQS) and to protect water systems from potentially harmful pollutants. In this sense, the European Union (EU) has been making efforts towards the implementation of EQS for priority substances, which were first set by Directive 2013/39/EU. This Directive, which also settled the necessity to develop a strategic approach to water contamination by pharmaceutical substances, established that future prioritization should be supported on the basis of results from Union-wide monitoring of emerging contaminants included in watch-lists that should be revised every two years. Several pharmaceuticals were included in a first watch-list (Decision 2015/495/EU), in the report by Loos et al. (2018) and also in a second watch-list (Decision 2018/840/EU), as for the significant risk that they may pose to or via the aquatic environment.

One of the main sources of pharmaceuticals in water systems is the discharge of wastewater treatment plants' (WWTPs) effluents into the environment (Yang et al., 2017). Generally, the wastewater treatment processes applied in WWTPs are inefficient in the removal of pharmaceuticals, and advanced tertiary treatments can be very costly to implement. Among the existing advanced treatments, adsorption by activated carbon (AC) is one of the most versatile, having the advantage of no by-products' generation. ACs are available in powder (PAC) or granular (GAC) forms, and the selection of the most adequate formulation depends on the type of reactor to be used. GAC is frequently applied in the removal of organic compounds from water and wastewater (de Franco et al., 2017) and it can be used both in stirred-tank and column (fixed-bed) reactors; yet, fixed-bed columns are the most common for treating wastewater with GAC (Metcalf & Eddy, 2003). This type

of reactor presents several advantages, namely, simple operation mode, effectiveness and easiness of scaling-up for industrial applications (de Franco et al., 2017). Therefore, fixed-bed studies are very important before planning the application of GAC in a treatment facility, allowing to determine the breakthrough curve and to obtain information for the design of the system, so to define a rational scale for practical operation (Pelech et al., 2006; Xu et al., 2013). After fixed-bed saturation, GAC can be subjected to regeneration (so minimizing the demand of virgin adsorbents), which may be advantageous in terms of economic viability, environmental and energetic sustainability (Radhika et al., 2018).

In the literature there are many studies on the adsorption of pharmaceuticals under batch operation in stirred reactors, using different adsorbents, which are mainly powdered materials. However, a smaller number of works have been published on the application of continuous fixed-bed adsorption in the removal of pharmaceuticals from water, highlighting the advantages, namely the high adsorption performance, flexibility, and capacity for adsorbent regeneration (Ahmed and Hameed, 2018). On the other hand, although some adsorbents from agriculture wastes (such as raspberry, olive stones, walnut shell, coffee residue or peach stones) have been used in fixed-bed adsorption of pharmaceuticals (Ahmed and Hameed, 2018), to the best of our knowledge, the utilization of industrial waste-based materials has not been yet assessed for this purpose.

In a previous study (Jaria et al., 2019), the production of a waste-derived GAC using two industrial residues, namely primary paper mill sludge (as raw material) and ammonium lignosulfonate (as binder agent), was achieved. The resulting material (PSA-PA) was shown to be efficient in the adsorption of pharmaceuticals from water in stirred reactors under batch operation conditions (Jaria et al., 2019). In the present study, PSA-PA has been packed in column reactors in order to assess the fixed-bed continuous adsorption

of three pharmaceuticals – the antiepileptic carbamazepine (CBZ), the antibiotic sulfamethoxazole (SMX), and antidepressant paroxetine (PAR) - from single and ternary solutions. These pharmaceuticals were selected due to their frequent occurrence in the aquatic environment, and potential harmful effects that they can pose to aquatic life (Ahlford, 2012, Ebele et al., 2017; Yang et al., 2017; Andrade et al., 2018). Also, they have different physico-chemical properties allowing to better assess the efficiency of the produced material towards compounds with different characteristics. In addition, the pharmaceuticals' adsorption was studied in two matrices (distilled water and final effluent of an urban WWTP), under different flow rates, and the thermal regeneration of PSA-PA was also fulfilled to evaluate its life cycle.

2. Experimental

2.1. Reagents

The pharmaceuticals used for the adsorption experiments were CBZ (carbamazepine, Sigma-Aldrich, 99%), SMX (sulfamethoxazole, TCI, >98%) and PAR (paroxetine-hydrochloride, TCI, >98%), which were prepared in distilled water or in wastewater (details on wastewater collection and characterization are presented in section 2.2. For the analytical quantification of the pharmaceuticals, all the chemicals used were of analytical grade: sodium hydroxide (Fluka), sodium dodecylsulphate (SDS, 99%, Sigma-Aldrich), hexadimetrine bromide (polybrene, Sigma-Aldrich), sodium tetraborate (Riedel-de-Haën), and ethylvanillin (99%, Sigma-Aldrich). Solutions were all prepared using ultrapure water, obtained from a Milli-Q Millipore system (Milli-Q plus 185).

2.2. Wastewater samples

Wastewater was collected from the outlet of a local WWTP, which serves 159 700 population equivalents and operates primary and biological treatments. The collected wastewater corresponds to the final effluent, after the biological treatment, as it is discharged into the receiving waters. Five collection campaigns were carried out between March and June 2018. Before use in the fixed-bed adsorption experiments, wastewater was filtered through 0.45 μm, 293 mm membrane filters (Gelman Sciences), immediately stored in dark at 4 ºC and used within no longer than 15 days.

After collection, wastewater was characterized by measuring conductivity (WTW meter), pH (pH/mV/°C meter pHenomenal® pH 1100L, VWR) and total organic carbon (Shimadzu, model TOC-V_{CPH}, SSM-5000A). Furthermore, the background concentration of the pharmaceuticals here considered in wastewater was determined according to the procedure described in section 2.4, being always below the detection limit. Characterization results are presented in Supplementary Material (SM) (Table S1), where it may be seen that the properties of the collected wastewater remained quite stable between campaigns.

2.3. Fixed-bed experiments

The adsorbent used in this work was a waste-derived GAC (PSA-PA) that was produced using two industrial residues: primary sludge (PS) resulting from pulp and paper manufacture, which was used as precursor, and ammonium lignosulfonate derived from the sulphite process applied in the production of cellulose pulp, which was used as binder agent. Every year, only in Portugal, about 300 000 tons of primary (~70%) and biologic (~30%) paper mill sludge are produced, being mostly managed through energetic valorization and landfilling (CELPA, 2017; Molina-Sánchez et al., 2018).

The production of PSA-PA consisted of a two-step pyrolysis combined with chemical activation and agglomeration of PS as is described in detail by Jaria et al., (2019), along with the physicochemical characterization of the resulting material. Briefly, the production of PSA-PA consisted of the mixture of dry PS with a 50% ammonium lignosulfonate solution in the ratio of 6:5 (*w*:*w*). This mixture was dried and pyrolysed at 500 ºC during 10 minutes under nitrogen atmosphere. The resultant material was then impregnated with a solution of potassium hydroxide (KOH) in the ratio 1:1 (*w*:*w*) and the impregnated carbon was then pyrolysed at 800 ºC during 150 minutes under nitrogen atmosphere. The material was washed with hydrochloric acid followed by distilled water and dried in an oven at 105 ºC for 24 h. Finally, the material was sieved and the granulometry 0.5 - 1.0 mm was selected.

The fixed-bed performance of PSA-PA in the removal of pharmaceuticals under continuous operation mode was evaluated using column reactors, as described in the following sub-sections. All the fixed-bed experiments were performed in a CHROMAFLEX® glass column (13 cm total height, 2.5 cm internal diameter), with an acrylic jacket, at a constant temperature of 25 ± 1 ^{o}C using a thermostatic recirculating bath (HAAKE A10, Thermo Scientific). The column was packed with PSA-PA with a constant bed depth (*Z*) of 2.6 cm, corresponding to 3.6 g of PSA-PA, using a flow adapter, with a 20 µm porosity HDPE bed support on the top of the column.

Before each experiment, the system was equilibrated for about 24 h with a continuous flow of distilled water. This time of equilibration was chosen according to the results obtained from an experiment where a PSA-PA fixed-bed column was fed with distilled water, at a flow rate of 4.3 L d^{-1}, and samples were collected from the outlet. The samples were analyzed in terms of conductivity (WTW meter) and TOC (Shimadzu, model

TOC-V_{CPH}, SSM-5000A). After 24 h of equilibration the conductivity and TOC values indicated the stability of the effluent, with negligible variations.

After equilibrating the system, the corresponding pharmaceutical(s) solution was up-flow pumped into the column with a peristaltic pump (BT100-2J/DG15-28, 2 channels, Longer Pump). Effluent samples were collected at set time intervals until the concentration of pharmaceutical remained constant by using a programmable fraction collector (IS-95 Interval Sampler, Spectra/Chrom®). The pharmaceuticals' concentration was determined according to the procedure described in section 2.4.

2.3.1. Fixed-bed adsorption of pharmaceuticals

Fixed-bed studies on the adsorptive removal of pharmaceuticals by PSA-PA under continuous operation mode were carried out in two subsequent stages:

i) Study of the effect of flow rate on the adsorption of CBZ using distilled water and wastewater as solvents. For this purpose, the fixed-bed column was fed with a single solution of CBZ (5 mg L^{-1}) at flow rates of 4.3, 8.4, and 13.0 L d^{-1}. CBZ solution was prepared either in distilled water or in wastewater and fed at the three different flow rates mentioned above.

ii) Study of the adsorption of CBZ, SMX and PAR from single (5 mg L^{-1}) or ternary (5 mg L^{-1} of each pharmaceutical) solutions in wastewater. These experiments were carried out at the most favorable flow rate (4.3 L d^{-1}), as selected from results obtained for CBZ in i).

2.3.2. Regeneration of exhausted PSA-PA adsorbent

Thermal regeneration of PSA-PA saturated with CBZ (after adsorption from distilled water) was performed at 500 ºC under nitrogen atmosphere for 90 min. The chosen temperature was based on the results from the thermogravimetric analysis (TGA) of CBZ, which indicates that this pharmaceutical is degraded around 300 ºC (Ullah et al., 2015). After regeneration, PSA-PA was packed into the column and the fixed-bed adsorption of CBZ, dissolved in distilled water, under a flow rate of 4.3 L d^{-1}, was determined (cycle 1). Subsequently, the exhausted regenerated PSA-PA was subjected to a second thermal regeneration and the fixed-bed adsorption was repeated using the same conditions (cycle 2). The specific surface area (S_{BET}) of the PSA-PA used in each fixed-bed adsorption cycle and of PSA-PA after the cycle 2 was determined by nitrogen adsorption isotherms, acquired at 77 K using a Micromeritics Instrument, Gemini VII 2380. The materials were outgassed overnight at 120 ºC. S_{BET} was calculated from the Brunauer–Emmett–Teller equation (Brunauer et al., 1938) in the relative pressure range 0.01–0.1. Pore volume (V_p) was estimated from the amount of nitrogen adsorbed at a relative pressure of 0.99 and micropore volume (W_0) was determined by applying the Dubinin-Radushkevich (DR) (Dubinin, 1966) or the Dubinin-Astakhov (DA) equations (Dubinin and Astakhov, 1971) to the lower relative pressure zone of the isotherm.

2.3.3. Fixed-bed column data analysis

To evaluate the adsorption of the pharmaceuticals onto PSA-PA in a fixed-bed system, breakthrough curves were obtained by plotting C/C_0 (where C is the concentration of the compound at the outlet of the column at a time t and C_0 is the initial concentration of the compound) as a function of operating time (t, min). Breakthrough curves allow to

determine the breakthrough point, which is the time when the effluent concentration reaches a determined percentage relatively to the influent concentration. This percentage can be defined according to legislated thresholds (when existent) or to an operator defined value, frequently between 5 and 10% (Metcalf & Eddy, 2003). The breakthrough point is an important parameter as it allows to determine the volume of treated effluent by the system (Ferreira et al., 2017). In the case of the pharmaceuticals here studied, no maximum limit is yet established for the discharge of these compounds into the environment, therefore, a 10% ($C/C_0 \approx 0.1$) was considered to define the breakthrough point ($t_{10\%}$).

The area above the total breakthrough curve allows to determine the bed adsorption capacity, q_{total} (mg g^{-1}) for a determined feed concentration (C_0, mg L^{-1}), calculated by:

$$q_{total} = \frac{Q}{1000}\frac{C_0 A}{m} = \frac{Q}{1000}\frac{C_0}{m}\int_{t=0}^{t=t_{total}}\left(1 - \frac{C}{C_0}\right)dt \qquad \text{Equation 1}$$

where Q is the flow rate (L d^{-1}); A is the area above the breakthrough curve; m is the dry weight of adsorbent in the column (g); C is the concentration of pharmaceutical at the outlet of the column at a time t (mg L^{-1}) and t_{total} is the total flow time (d) (Ferreira et al., 2017).

The height of the mass transfer zone (h_{MTZ}) is used as a parameter to select the best operating flow rate since the lowest the h_{MTZ}, the closer is the system to ideality (Lima et al., 2017). The calculation of h_{MTZ} is done by the following expression:

$$h_{MTZ} = \left(1 - \frac{q_t}{q_s}\right)h \qquad \text{Equation 2}$$

where q_t is the mass of adsorbate adsorbed at time t per gram of adsorbent (mg g^{-1}), q_s is the maximum mass of adsorbent adsorbed at saturation per gram of adsorbent (mg g^{-1}) and h is the bed height (cm).

Also, the empty bed contact time (EBCT), the adsorbent usage rate (U_r), and the fraction of bed utilization (FBU) are useful parameters for the analysis of breakthrough

curves. FBU is related to h_{MTZ}, and EBCT or residence time influences the volume of influent treated and the nature of the breakthrough curve (Deokar and Mandavgane, 2015). The expressions used for the calculation of the referred parameters are as follows:

$$EBCT = \frac{V_c}{Q} \qquad \text{Equation 3}$$

$$U_r = \frac{m}{V_b} \qquad \text{Equation 4}$$

$$FBU = \frac{q_b}{q_s} \qquad \text{Equation 5}$$

where V_c is the fixed-bed volume (L); Q is the flow rate (L d^{-1}); V_b is the volume treated at breakthrough (L); m is the mass of adsorbent (g);and q_b is the mass of adsorbate adsorbed per gram of adsorbent at breakthrough time ($t_{10\%}$), equivalent to $q_{10\%}$ (mg g^{-1}) (Deokar and Mandavgane, 2015)..

2.3.4. Mathematical breakthrough fitting models

In this work, three models were considered for describing the experimental breakthrough curves. The fittings were performed using GraphPad Prism 5.

Thomas model

The Thomas model (Thomas, 1944) assumes that the adsorption rate is described by a Langmuir adsorption kinetics, ignoring intraparticle (solid) mass transfer resistance, external fluid-film resistance and axial dispersion in the fixed-bed (de Franco et al., 2017; Ferreira et al., 2017; Sánchez-Machado et al., 2016). This model is represented by:

$$\frac{C}{C_0} = \frac{1}{1+exp\left(\frac{k_{TH}}{Q}(q_{TH}m - C_0Qt)\right)} \qquad \text{Equation 6}$$

where k_{TH} is the Thomas model rate constant (L d^{-1} mg^{-1}) and q_{TH} is the theoretical saturation adsorption capacity (mg g^{-1}).

Yoon-Nelson model

The Yoon-Nelson model intends to minimize the error associated to the Thomas model at small or high periods of time of the breakthrough curve (Singh and Thakur, 2016). It assumes that the decrease rate in the probability of adsorption of the adsorbate is proportional to the probability of the adsorbate adsorption and the probability of adsorbate breakthrough on the adsorbent (Deokar and Mandavgane, 2015; Singh and Thakur, 2016). The model is described by the following equation:

$$\frac{C}{C_0} = \frac{e\exp(k_{YN}t - t_{50\%}k_{YN})}{1 + e\exp(k_{YN}t - t_{50\%}k_{YN})} \qquad \text{Equation 7}$$

where k_{YN} is the Yoon-Nelson model rate constant (d^{-1}) and $t_{50\%}$ is the time (d) required for 50% of the adsorbate breakthroughs (Singh and Thakur, 2016).

Yan Model

Yan model, also known as Modified Dose Response (MDR), was developed by Yan et al. (2001), in order to minimize the deviation between experimental data and the predicted breakthrough curve from Thomas model, especially when very small or very large operation times are needed (de Franco et al., 2017). The model is described by the following expression:

$$\frac{C}{C_0} = 1 - \frac{1}{1 + \left(\frac{C_0 Q t}{q_Y m}\right)^{\alpha^Y}} \qquad \text{Equation 8}$$

where q_Y is the amount of solute adsorbed (mg g^{-1}) and α^Y is a model parameter (de Franco et al., 2017; Xu et al., 2013).

2.4. Quantification of pharmaceuticals

The concentration of the pharmaceuticals in the column effluent was determined by capillary electrophoresis using a micellar electrokinetic chromatography (MEKC) method, in a Beckman P/ACE MDQ instrument (Fullerton, CA, USA), equipped with a UV detector, as described by Jaria et al. (2019). Briefly, a fused-silica capillary with a total length of 40 cm (30 cm to detector) and 75 μm of internal diameter was coated following the next steps: 1 M NaOH solution for 30 min; ultrapure water for 15 min; hexadimethrine bromide (polybrene) 0.5% (*w/v*) in 0.5 M NaCl for 20 min; ultrapure water for 2 min; and, finally, running buffer for 20 min. The running buffer used consisted of 15 mM of sodium tetraborate and 30 mM of sodium dodecyl sulfate. Before each run, the capillary was flushed with ultrapure water for 1 min and running buffer solution for 1.5 min. The coating and washing steps were performed at 20 psi. The pharmaceutical standard solutions were prepared with a final concentration of 5 mg L^{-1} and a stock solution of ethylvanillin was used as internal standard. CBZ was analyzed at 214 nm, while SMX and PAR were determined at 200 nm.

3. Results and Discussion

3.1. Fixed-bed adsorption of pharmaceuticals onto PSA-PA

3.1.1. Adsorption of CBZ from distilled water and wastewater at different flow rates

The experimental breakthrough curves of the fixed-bed adsorption of CBZ onto PSA-PA from distilled water and wastewater are presented in Figure 1. The breakthrough

curves represent the ratio of concentration at a time *t* and the initial concentration (C/C_0) *versus* time (in days).

The results displayed in Figure 1 show that fixed-bed adsorption of CBZ onto PSA-PA was affected by the flow rate and the aqueous matrix. As it may be seen, in both matrices, the largest the flow rate, the steeper the breakthrough curve. This may be due to the fact that the increase in the flow rate implies a lessening of the contact time between the adsorbent (PSA-PA) and the adsorbate (CBZ), which leads to a reduction in the bed adsorption capacity and service time. With respect to the matrix, steeper curves were determined in wastewater than in distilled water, which must be associated with competition effects in wastewater. On the other hand, as it may be seen in Figure 1, asymmetric breakthrough curves were obtained under the experimental conditions used. The breakthrough curves are skewed and steeper at the initial part of the experiment, which may be associated, at least partially, to heterogeneity within the bed. Even small differences in the particle size of the granular PSA-PA may result in some heterogeneity in packing densities within the bed. Furthermore, the shape of the breakthrough curves is highly influenced by the adsorption rate or mass transfer from the aqueous phase to the adsorption sites inside the PSA-PA particles. Curves in Figure 1 show that, especially at the highest flow rate, breakthrough occurs very quickly, and it is almost spontaneous, which indicates that the CBZ molecules move through the packed bed and reach the outlet before they can enter the pores of the PSA-PA particles. Then, the exhaustion of the bed ($C/C_0 = 1$) is not attained within the duration of the experiments. This behavior has already been observed by other authors in fixed-bed studies involving the adsorption of pharmaceuticals (Darweesh and Ahmed, 2017; Nazari et al., 2016). In this specific study, such a pattern must be related

to the slow adsorption kinetics of CBZ onto PSA-PA, which possesses very narrow pores (Jaria et al., 2019).

Efficiency and mass transfer parameters derived from experimental breakthrough curves on the fixed-bed adsorption of CBZ from distilled and wastewater are presented in Table 1. These parameters evidence that, for both aqueous matrices, the lowest flow rate (4.3 L d^{-1}) is the one presenting a longer operation time (breakthrough time), defined as the time for which 10% of saturation ($t_{10\%}$) of the adsorbent is attained, and a larger treated volume. Also, at this flow rate (4.3 L d^{-1}), FBU, which express the relation between the amount of CBZ adsorbed at breakthrough point and at saturation, is higher. By increasing the flow rate, a decrease in $t_{10\%}$ and in the total mass of CBZ adsorbed onto PSA-PA (q_{total}) is obtained. In fact, the correlations between the flow rates and these two parameters are quite linear, except for q_{total} in wastewater, which at the flow rates of 4.3 and 8.6 L d^{-1} is quite similar, but notoriously decreases at 13.0 L d^{-1}. The decrease in the q_{total} and $t_{10\%}$ with the increase in the flow rate can be attributed to the insufficient contact time between the CBZ and PSA-PA, which has already been observed in other systems (Deokar and Mandavgane, 2015; Tor et al., 2009). The h_{MTZ} value is equal to the fixed-bed height under the three different flow rates and in the two aqueous matrices, which further confirms that CBZ molecules move quickly towards the outlet of the column. Concerning U_r, its value increases with the increase in the flow rate: in wastewater, this increase is very accentuated, being 10 times higher when changing from a flow rate of 8.6 to 13.0 L d^{-1}. According to Sánchez-Machado et al. (2016), high flow rates reduce the thickness of liquid film around adsorbent particles leading to low mass transfer resistance and high rate of mass transfer, explaining the increase in *Ur* with the increase in the flow rate.

Table 2 depicts the parameters from the fittings of breakthrough experimental curves in Figure 1 to the considered models. As evidenced by the R^2, the Yan model is the one that best fits the fixed-bed adsorption of CBZ onto PSA-PA at the three flow rates and both in distilled and wastewater matrices. Fittings to the Yan model are shown together with experimental results in Figure 1, while, for comparison purposes, fittings to the three models here considered are represented in Figures S1 and S2 in SM (please, note that the fittings to the Thomas and Yoon-Nelson are superimposed in Figures S1 and S2). Regarding parameters in Table 2, the predicted values for the maximum adsorption capacity determined by the Thomas and the Yan models (q_{Th} and q_Y, respectively) are, except for Q = 13.0 L d^{-1} in wastewater, quite higher than the experimentally calculated one (q_{total} in Table 1). In any case, q_Y is, as expected due to the best fitting, closer to the experimentally calculated values than q_{Th}, especially in distilled water. Comparing the values of the batch studies (Jaria et al., 2019) with these results, it may be seen that for CBZ in distilled water, the maximum adsorption capacity at saturation in batch system (q_m = 24 ± 5 mg g^{-1}) is less than half of that estimated by the Yan model for the continuous system at Q = 4.3 L d^{-1} (q_Y = 59.6 ± 0.6 mg g^{-1}). In wastewater matrix, the difference is not so accentuated, with q_m = 10 ± 1 mg g^{-1} for batch system (Jaria et al., 2019) and q_Y =12.5 ± 0.4 mg g^{-1} for the fixed-bed column. The same tendency is verified for Q = 8.6 mL min^{-1}. According to Tor et al. (2009), differences on maximum adsorption capacities between batch and continuous modes, for the same initial concentration of adsorbate, have been observed in other studies and they may be due to the textural properties of the adsorbent, namely the characteristics of the porous structure. In this case, the microporous structure of PSA-PA may lead to difficulties in the retention of CBZ molecules under the fixed-bed experimental conditions used.

As referred, Yan model is the one that best describes the adsorption of CBZ onto PSA-PA in the studied fixed-bed continuous adsorption systems. However, apart from the maximum adsorption capacity, no other theoretical information can be deduced from the model. On the other hand, Thomas model allows to observe that the predicted adsorption rate constant increases with increasing flow rate, meaning that the mass transfer resistance decreases and, proportionally, the axial dispersion and thickness of the liquid film on the particle surface also decrease (Tor et al., 2009). Additionally, the Yoon-Nelson model gives the predicted time for the 50% of fixed-bed saturation ($t_{50\%}$) which is, for CBZ in distilled water, very close to the experimental values, only showing a variation between 5 and 16% relatively to the experimental value (Table 2). For wastewater, the differences are greater, with $t_{50\%}$ being highly overestimated by the model, except for the flow rate of 13.0 L d^{-1}.

Considering the obtained results for the fixed-bed adsorption of CBZ onto PSA-PA, the flow rate of 4.3 L d^{-1} was chosen as the most favorable in terms of $t_{10\%}$, FBU and U_r, and hence used in the subsequent experiments in wastewater.

3.1.2. Adsorption of CBZ, SMX, and PAR from single and ternary solutions in wastewater

The experimental breakthrough curves on the adsorption of CBZ, SMX and PAR from their single and ternary wastewater solutions are presented in Figure 2 a) and b), respectively. Regarding the single adsorption, it is evident that the breakthrough curve for SMX is steeper than those of PAR and CBZ. Still, the initial elution of PAR from the PSA-PA packed bed is almost immediate, while that of CBZ and SMX takes a bit longer. As already mentioned for CBZ, under the used experimental conditions, the fast elution together with asymmetric skewed curves not reaching exhaustion within the duration of the experiments point to adsorption kinetic limitations in the retention of these pharmaceuticals

in the PSA-PA active sites. Also, in the wastewater matrix and, particularly, in the case of PAR, some biodegradation might be occurring simultaneously with adsorption, meaning further depletion of the pharmaceuticals' concentration (Metcalf & Eddy, 2003). This hypothesis is mainly viable for PAR once this pharmaceutical is liable to degrade by autochthonous microorganisms present in activated sludge and estuarine sediments (Duarte et al., 2019). Regarding the adsorption of the considered pharmaceuticals from their ternary solution in wastewater (Figure 2 b)), and comparatively with their respective single adsorption (Figure 2 a)), steeper and higher breakthrough curves were obtained for CBZ and SMX while the contrary was observed for PAR.

Efficiency and mass transfer parameters in Table 1 evidence that, for the single adsorption, in wastewater, the breakthrough time ($t_{10\%}$) and the corresponding adsorption capacity ($q_{10\%}$) of each pharmaceutical are very distinct, diminishing in the order CBZ > SMX > PAR. This must be related to the almost spontaneous elution of PAR from the PSA-PA fixed-bed. However, the order of the total mass adsorbed (q_{total}) does not coincide with the breakthrough order, with PSA-PA showing greater adsorption for CBZ, followed by PAR and SMX. The latter is in agreement with previous results obtained under batch conditions (Jaria et al., 2019), which pointed to the relatively low SMX adsorption capacity of PSA-PA in wastewater (as compared with CBZ and PAR). This was related with the pH of wastewater, which implies a negative charge for both PSA-PA and SMX, leading to some electrostatic repulsion between adsorbate and adsorbent (Jaria et al., 2019). This, together with competitive and possible exclusion effects (due to the high presence of pores below 5 nm and a low presence of mesoporosity in PSA-PA), might have also negatively affected the adsorption of PAR from the ternary solution. In fact, under competition with other pharmaceuticals in the ternary solution, the $t_{10\%}$ determined for PAR was zero, with

$t_{10\%}$ decreasing relatively to the single solution also for SMX and, especially, for CBZ. Interestingly, the largest capacity (q_{total}) for the adsorption from the ternary solution was obtained for PAR, followed by CBZ, and then by SMX. This behavior can be explained by the slower adsorption kinetics of PAR adsorption onto PSA-PA compared to CBZ and SMX, as observed in the batch stirred system by Jaria et al. (2019). Concerning U_r determined for the fixed-bed adsorption from wastewater single solution, its value increases in the order CBZ < SMX < PAR, as well as for the corresponding decreasing volume treated at the breakthrough (V_b). Adsorption from the ternary solution meant a notorious decrease in the volume treated at breakthrough, V_b, for the three pharmaceuticals, increasing in the order PAR < CBZ < SMX. In the case of ternary solution, this may be related with competitive effects, which resulted in a lower U_r value for SMX than for CBZ.

The parameters from the fitting of the experimental results to the considered mathematical models for the adsorption of CBZ, SMX and PAR from their single and ternary solutions in wastewater are depicted in Table 3. As for the corresponding R^2, it is evident that the Yan model continues to be the model that best describes the experimental data and the corresponding fittings are shown together with experimental results in Figure 2. For comparison purposes, fittings to the three models here considered are displayed along with experimental results in Figure S3 and S4 in SM (please, note that fittings to the Thomas and Yoon-Nelson models are superimposed). Regarding the fitting parameters (Table 3), it is to highlight that the q_Y for the fixed-bed adsorption from single solution is overestimated as compared with the experimental maximum adsorption capacity (q_{total} in Table 1) for CBZ, SMX and PAR. However, for adsorption from the ternary solution, q_Y is slightly smaller than q_{total} for CBZ, while it is larger than q_{total} for PAR and, especially, for

SMX. Divergences are possibly related to deviations of the Yan fitting from experimental results at the end of the experimental curve, which does not reach exhaustion.

3.2. Regeneration and adsorption onto regenerated PSA-PA

The experimental breakthrough curves corresponding to the fixed-bed adsorption of CBZ onto PSA-PA (Q = 4.3 L d^{-1}) in subsequent cycles after regeneration are depicted in Figure 3. As it may be seen, steeper curves are obtained from cycle 0 to cycle 2, accompanied by a reduction of the PSA-PA capacity during regeneration. This is further confirmed by the corresponding efficiency and mass transfer parameters in Table 1. Observing the parameters for the cycles 0 (virgin PSA-PA), 1 (after first regeneration) and 2 (after second regeneration), it is possible to see that the $q_{10\%}$ was reduced by 39 and 86%, while the q_{total} decreased in 38 and 71%, after regeneration cycles 1 and 2, respectively. This decrease in the adsorption capacity of the regenerated PSA-PA may be related to a decrease in the S_{BET} after the thermal regeneration. Table 4 presents the textural parameters of the virgin and regenerated PSA-PA used in the subsequent cycles and of the exhausted PSA-PA after use in cycle 2. These results show a decrease in the S_{BET} after regeneration, which is more notorious after the second thermal regeneration. Also, a decrease of the total pore volume (V_p) and the micropore volume (W_0) may be observed after regeneration, and especially after the second thermal regeneration. Meanwhile, the average pore diameter (D) and average pore width (L) increase in the subsequent thermal regeneration treatments, due to the destruction of the micropore structure of the adsorbent. Still, the decrease in S_{BET} and W_0, is not so relevant as the adsorption capacity reduction, especially in the cycle 1, which indicates that other factors are probably affecting the adsorption of CBZ in subsequent cycles. For instance, a change in the surface functionality of the regenerated adsorbent

could be also an important factor influencing the results, since it was already observed that chemical interactions are determinant in the adsorption of CBZ onto PSA-PA (Jaria et al., 2019).

Parameters corresponding to the fittings of the experimental breakthrough curves to the Thomas, Yoon-Nelson and Yan models are depicted in Table 5. As for the largest R^2, the Yan model is again the one providing the best fittings, which are shown in Figure 3 together with the experimental results. For comparison purposes, Figure S5 (SM) represents the fittings to the three models considered (note that fittings to Thomas and Yoon-Nelson models are superimposed). Regarding the q_Y, values in Table 5 overestimate the experimental q_{total} values in Table 1. Anyhow, the q_Y values further confirm the depletion of the CBZ adsorption capacity in subsequent utilization cycles after PSA-PA thermal regeneration.

Based on the above-mentioned results, not more than one cycle of utilization of PSA-PA after regeneration should be set taking into account the energy consumption associated to thermal regeneration together with the loss of adsorption capacity. Moreover, given that the production of PSA-PA is based on the use of two residues as raw materials, obtaining new PSA-PA could be also equated.

4. Comparison with other studies assessing the removal of CBZ, SMX and PAR in fixed-bed reactors

To the best of authors' knowledge, only a few studies evaluated the adsorptive removal of CBZ and SMX in fixed-bed reactors, with most of studies being focused on the adsorption in batch mode. Moreover, in relation to PAR, there are no literature data on its adsorption in fixed-bed systems. Furthermore, the existing works concerning the adsorption

of pharmaceuticals onto AC using fixed-bed reactors were carried out under very distinct operational conditions, making extremely difficult to establish valid comparisons between them (Ahmed and Hameed, 2018; Ek et al., 2014; Hu et al., 2016; Sotelo et al., 2013; Sperlich et al., 2017; Torrellas et al., 2015; Yu et al., 2009; Zuo et al., 2016). Notwithstanding, some of the most relevant studies are commented below.

Zuo et al. (2016) used three carbon adsorbents (including a commercial PAC) in a fixed-bed system for the removal of SMX from solution, using columns packed with 27 g of adsorbent (mixed with quartz sand). The amount of SMX adsorbed onto the studied PAC at saturation time was 846 mmol kg^{-1}, corresponding to 214.29 mg g^{-1}. The adsorption of SMX and CBZ onto a PAC in a fixed-bed system for application as wastewater tertiary treatment was also evaluated by Hu et al. (2016).

Concerning the use of GACs in fixed-bed reactors, Sotelo et al. (2013), Sperlich et al. (2017), and Yu et al. (2009) addressed the adsorptive removal of CBZ from water using commercial GACs, while Torrellas et al. (2015) used a GAC produced from peach stones activated with H_3PO_4. In the latter study, 0.6 g of three GACs (the originally produced from the peach stones percursor with H_3PO_4 activation, and two that were subsequently obtained from the modification of the original) were used. The operational conditions applied consisted in an initial concentration of 15 mg L^{-1} CBZ and a flow rate of 3 mL min^{-1} (corresponding to a flow rate of 4.3 L d^{-1}, used in this study), and the amount of CBZ adsorbed at breakthrough time varied between 5.8 mg g^{-1} and 24.4 mg g^{-1} with the breakthrough times obtained from C/C_0 of 0.30 and 0.52. The total amount adsorbed (at saturation time) varied between 69.7 mg g^{-1} and 235.1 mg g^{-1}. In a work performed by Ek et al. (2014), a pilot study for the application of sequential column reactors, using commercial

GACs for wastewater treatment was studied, and CBZ was one of the emerging contaminants addressed, using environmentally realistic concentrations.

Other studies refer to the removal of CBZ and SMX in fixed-bed systems, however with other adsorbent materials than ACs, such as resins (Wang et al., 2016), montmorillonite modified with ionic liquid (Lawal and Moodley, 2018), modified Y-zeolites (Cabrera-Lafaurie et al., 2015,2014), and carbon nanotubes (Tian et al., 2013). Besides the scarcity of publications regarding the adsorption of these pharmaceuticals in fixed-bed reactors, the use of industrial residues as precursors for the production of a GAC to be used in these systems is, as far as it concerns the authors' knowledge, inexistent.

5. Conclusions

The fixed-bed adsorption performance of CBZ using PSA-PA, a primary paper mill sludge-based GAC, was greater in distilled water than in wastewater, possibly due to the competitive effects in the latter. In both matrices, the larger the flow rate, the steeper the breakthrough curves, with the most favorable flow rate being 4.3 L d^{-1}. Under this flow rate, the fixed-bed adsorption of CBZ, SMX and PAR from their single solution in wastewater showed that the bed capacity decreased in the order CBZ > PAR > SMX. However, from the ternary solution, it decreased following the order PAR > CBZ > SMX since the bed capacity for CBZ and, especially, for SMX decreased under the competition of the other pharmaceuticals. Contrarily, and despite being eluted instantaneously from the column, PAR showed an enhanced bed capacity in the ternary solution. The Yan model was the one that generally best described the experimental breakthrough curves for the adsorption of the considered pharmaceuticals under the tested experimental conditions. Finally, although the thermal regeneration of PSA-PA involved a relatively low decrease in

its S_{BET}, it resulted in a reduction of the CBZ bed adsorption capacity of around 39 and 71% in the first and second regeneration stages, respectively. Therefore, no more than one regeneration stage is recommended for the fixed-bed utilization of PSA-PA in the removal of CBZ.

Studies assessing the removal of these pharmaceuticals using GAC produced from industrial residues in fixed-bed systems are very scarce and, therefore, the present study is a relevant contribution to this field.

Acknowledgments

This work is a contribution to the project RemPharm (PTDC/AAG-TEC/1762/2014) funded by FCT – Fundação para a Ciência e a Tecnologia, I.P., through national funds, and the co-funding by the FEDER, within the PT2020 Partnership Agreement and Compete 2020. Thanks are also due for the financial support to CESAM (UID/AMB/50017/2019), to FCT/MEC through national funds, and the co-funding by the FEDER, within the PT2020 Partnership Agreement and Compete 2020. Vânia Calisto and Guilaine Jaria thank FCT for their grants (SFRH/BPD/78645/2011 and SFRH/BD/138388/2018, respectively); Marta Otero and Vânia Calisto are also thankful to FCT for the Investigator Program (IF/00314/2015) and the Scientific Employment Stimulus (CEECIND/00007/2017), respectively. Milton Fontes and workers of Aveiro's WWTP (Águas do Centro Litoral, Portugal) are gratefully acknowledged for assistance on the effluent sampling campaigns.

5. References

Ahlford, K., 2012. Environmental Risk Assessment of Selective Serotonin Reuptake Inhibitors (SSRIs) Fluoxetine, Citalopram, Sertraline, Paroxetine and the Benzodiazepine Oxazepam. In https://www.ibg.uu.se/digitalAssets/177/c_177014-l_3-k_ahlford-kristina-report.pdf.

Ahmed, M.J., Hameed, B.H., 2018. Removal of emerging pharmaceutical contaminants by adsorption in a fixed-bed column: A review. Ecotoxicol. Environ. Saf. 149, 257–266. https://doi.org/10.1016/j.ecoenv.2017.12.012

Andrade, J.R., Oliveira, M.F., Da Silva, M.G.C., Vieira, M.G.A., 2018. Adsorption of Pharmaceuticals from Water and Wastewater Using Nonconventional Low-Cost Materials: A Review. Industrial and Engineering Chemistry Research 57, 3103-3127.

Associação da Indústria Papeleira (CELPA), 2017. Boletim Estatístico Indústria Papeleira Portuguesa. In http://www.celpa.pt/wp-content/uploads/2018/10/Boletim_WEB-2.pdf. Accessed in (April 2019)

Brunauer, S., Emmett, P.H., Teller, E., 1938. Adsorption of gases in multimolecular layers, J. Am. Chem. Soc., 60.

Cabrera-Lafaurie, W.A., Román, F.R., Hernández-Maldonado, A.J., 2014. Removal of salicylic acid and carbamazepine from aqueous solution with Y-zeolites modified with extraframework transition metal and surfactant cations: Equilibrium and fixed-bed adsorption. J. Environ. Chem. Eng. 2, 899–906. https://doi.org/10.1016/j.jece.2014.02.008

Cabrera-Lafaurie, W.A., Román, F.R., Hernández-Maldonado, A.J., 2015. Single and multi-component adsorption of salicylic acid, clofibric acid, carbamazepine and caffeine from water onto transition metal modified and partially calcined inorganic-

organic pillared clay fixed beds. J. Hazard. Mater. 282, 174–182. https://doi.org/10.1016/j.jhazmat.2014.03.009

Commission Implementing Decision (EU) 2015/495 of 20 March 2015 establishing a watch list of substances for Union-wide monitoring in the field of water policy pursuant to Directive 2008/105/EC of the European Parliament and of the Council (notified under document C(2015) 1756).

Commission Implementing Decision (EU) 2018/840 of 5 June 2018 establishing a watch list substances for Union-wide monitoring in the field of water policy pursuant to Directive 2008/105/EC of the European Parliament and of the Council and repealing Commission Implementing Decision (EU) 2015/495 (notified under document C(2018) 3362).

Darweesh, T.M., Ahmed, M.J., 2017. Adsorption of ciprofloxacin and norfloxacin from aqueous solution onto granular activated carbon in fixed bed column. Ecotoxicol. Environ. Saf. 138, 139–145. https://doi.org/10.1016/j.ecoenv.2016.12.032

de Franco, M.A.E., de Carvalho, C.B., Bonetto, M.M., Soares, R. de P., Féris, L.A., 2017. Removal of amoxicillin from water by adsorption onto activated carbon in batch process and fixed bed column: Kinetics, isotherms, experimental design and breakthrough curves modelling. J. Clean. Prod. 161, 947–956. https://doi.org/10.1016/j.jclepro.2017.05.197

Deokar, S.K., Mandavgane, S.A., 2015. Estimation of packed-bed parameters and prediction of breakthrough curves for adsorptive removal of 2,4-dichlorophenoxyacetic acid using rice husk ash. J. Environ. Chem. Eng. 3, 1827–1836. https://doi.org/10.1016/j.jece.2015.06.025

Duarte, P., Almeida, C.M.R., Fernandes, J.P., Morais, D., Lino, M., Gomes, C.R., Carvalho, M.F., Mucha, A.P., 2019. Bioremediation of bezafibrate and paroxetine by microorganisms from estuarine sediment and activated sludge of an associated wastewater treatment plant. Sci. Total Environ. 655, 796–806. https://doi.org/10.1016/J.SCITOTENV.2018.11.285

Dubinin, M.M., 1966. Properties of active carbons. In: Chemistry and Physics of Carbon. Marcel Dekker Inc., New York, pp. 51–120.

Dubinin, M.M., Astakhov, V.A., 1971. Description of Adsorption Equilibria of Vapors on Zeolites over Wide Ranges of Temperature and Pressure. Adv. Chem., 102, 69–85.

Ebele, A.J., Abou-Elwafa Abdallah, M., Harrad, S., 2017. Pharmaceuticals and personal care products (PPCPs) in the freshwater aquatic environment. Emerging Contaminants 3, 1-16.

Ek, M., Baresel, C., Magnér, J., Bergstrom̈, R., Harding, M., 2014. Activated carbon for the removal of pharmaceutical residues from treated wastewater. Water Sci. Technol. 69, 2372–2380. https://doi.org/10.2166/wst.2014.172

European Parliament, Directive 2013/39/EU of the European Parliament and of the Council of 12 August 2013 amending Directives 2000/60/EC and 2008/105/EC as regards priority substances in the field of water policy, Official Journal of the European Union, (2013).

Ferreira, C.I.A., Calisto, V., Otero, M., Nadais, H., Esteves, V.I., 2017. Fixed-bed adsorption of Tricaine Methanesulfonate onto pyrolysed paper mill sludge. Aquac. Eng. 77, 53–60. https://doi.org/10.1016/j.aquaeng.2017.02.006

Hu, J., Aarts, A., Shang, R., Heijman, B., Rietveld, L., 2016. Integrating powdered activated carbon into wastewater tertiary filter for micro-pollutant removal. J. Environ. Manage. 177, 45–52. https://doi.org/10.1016/j.jenvman.2016.04.003

Jaria, G., Calisto, V., Silva, C.P., Gil, M.V., Otero, M., Esteves, V.I., 2019. Obtaining granular activated carbon from paper mill sludge – A challenge for application in the removal of pharmaceuticals from wastewater. Sci. Total Environ. 653, 393–400. https://doi.org/10.1016/J.SCITOTENV.2018.10.346

Lawal, I.A., Moodley, B., 2018. Fixed-Bed and Batch Adsorption of Pharmaceuticals from Aqueous Solutions on Ionic Liquid-Modified Montmorillonite. Chem. Eng. Technol. 41, 983–993. https://doi.org/10.1002/ceat.201700107

Lima, L.F., de Andrade, J.R., da Silva, M.G.C., Vieira, M.G.A., 2017. Fixed Bed Adsorption of Benzene, Toluene, and Xylene (BTX) Contaminants from Monocomponent and Multicomponent Solutions Using a Commercial Organoclay. Ind. Eng. Chem. Res. 56, 6326–6336. https://doi.org/10.1021/acs.iecr.7b00173

Loos, R., Marinov, D., Sanseverino, I., Napierska, D., and Lettieri, T., 2018. Review of the 1st Watch List under the Water Framework Directive and recommendations for the 2nd Watch List, EUR 29173 EN, Publications Office of the European Union, Luxembourg, ISBN 978-92-79-81839-4, doi:10.2760/614367, JRC111198

Metcalf & Eddy, I., 2003. Wastewater Engineering: Treatment and Reuse, Fourth. ed. McGraw-Hill.

Molina-Sánchez, E., Leyva-Díaz, J., Cortés-García, F., Molina-Moreno, V., 2018. Proposal of Sustainability Indicators for the Waste Management from the Paper Industry within the Circular Economy Model. Water 10, 1014. doi:10.3390/w10081014

Nazari, G., Abolghasemi, H., Esmaieli, M., Sadeghi Pouya, E., 2016. Aqueous phase adsorption of cephalexin by walnut shell-based activated carbon: A fixed-bed column study. Appl. Surf. Sci. 375, 144–153. https://doi.org/10.1016/J.APSUSC.2016.03.096

Pełech, R., Milchert, E., Bartkowiak, M., 2006. Fixed-bed adsorption of chlorinated hydrocarbons from multicomponent aqueous solution onto activated carbon: Equilibrium column model. J. Colloid Interface Sci. 296, 458–464. https://doi.org/10.1016/J.JCIS.2005.09.020

Radhika, R., Jayalatha, T., Rekha Krishnan, G., Jacob, S., Rajeev, R., George, B.K., 2018. Adsorption performance of packed bed column for the removal of perchlorate using modified activated carbon. Process Saf. Environ. Prot. 117, 350–362. https://doi.org/10.1016/J.PSEP.2018.04.026

Sánchez-Machado, D.I., López-Cervantes, J., Correa-Murrieta, M.A., Sánchez-Duarte, R.G., 2016. Modeling of breakthrough curves for aqueous iron (III) adsorption on chitosan-sodium tripolyphosphate. Water Sci. Technol. 74, 2297–2304. https://doi.org/10.2166/wst.2016.409

Singh, B., Thakur, V., 2016. Eco-friendly and Cost-effective Use of Rice Straw in the Form of Fixed Bed Column to Remove Water Pollutants. J. Bioremediation Biodegrad. 07. https://doi.org/10.4172/2155-6199.1000374

Sotelo, J.L., Ovejero, G., Rodríguez, A., Álvarez, S., García, J., 2013. Adsorption of Carbamazepine in Fixed Bed Columns: Experimental and Modeling Studies. Sep. Sci. Technol. 48, 2626–2637. https://doi.org/10.1080/01496395.2013.808215

Sperlich, A., Harder, M., Zietzschmann, F., Gnirss, R., 2017. Fate of trace organic compounds in granular activated carbon (GAC) adsorbers for drinking water treatment. Water (Switzerland) 9. https://doi.org/10.3390/w9070479

Thomas, H.C., 1944. Heterogeneous ion exchange in a flowing system. J. Am. Chem. Soc. 66, 1664–1666.

Tian, Y., Gao, B., Morales, V.L., Chen, H., Wang, Y., Li, H., 2013. Removal of sulfamethoxazole and sulfapyridine by carbon nanotubes in fixed-bed columns. Chemosphere 90, 2597–2605. https://doi.org/10.1016/j.chemosphere.2012.11.010

Tor, A., Danaoglu, N., Arslan, G., Cengeloglu, Y., 2009. Removal of fluoride from water by using granular red mud: Batch and column studies. J. Hazard. Mater. 164, 271–278. https://doi.org/10.1016/J.JHAZMAT.2008.08.011

Torrellas, S.Á., García Lovera, R., Escalona, N., Sepúlveda, C., Sotelo, J.L., García, J., 2015. Chemical-activated carbons from peach stones for the adsorption of emerging contaminants in aqueous solutions. Chem. Eng. J. 279, 788–798. https://doi.org/10.1016/j.cej.2015.05.104

Ullah, M., Ullah, H., Murtaza, G., Mahmood, Q., Hussain, I., 2015. Evaluation of influence of various polymers on dissolution and phase behavior of carbamazepine-succinic acid cocrystal in matrix tablets. Biomed Res. Int. 2015. https://doi.org/10.1155/2015/870656

Wang, W., Li, X., Yuan, S., Sun, J., Zheng, S., 2016. Effect of resin charged functional group, porosity, and chemical matrix on the long-term pharmaceutical removal mechanism by conventional ion exchange resins. Chemosphere 160, 71–79. https://doi.org/10.1016/j.chemosphere.2016.06.073

Xu, Z., Cai, J., Pan, B., 2013. Mathematically modeling fixed-bed adsorption in aqueous systems. J. Zhejiang Univ. Sci. A 14, 155–176. https://doi.org/10.1631/jzus.A1300029

Yan, G., Viraraghavan, T., Chen, M., 2001. A New Model for Heavy Metal Removal in a Biosorption Column. Adsorpt. Sci. Technol. 19, 25–43. https://doi.org/10.1260/0263617011493953

Yang, Y., Ok, Y.S., Kim, K.H., Kwon, E.E., Tsang, Y.F., 2017. Occurrences and removal of pharmaceuticals and personal care products (PPCPs) in drinking water and water/sewage treatment plants: A review. Sci. Total Environ. 596–597, 303–320. https://doi.org/10.1016/j.scitotenv.2017.04.102

Yu, Z., Peldszus, S., Huck, P.M., 2009. Adsorption of Selected Pharmaceuticals and an Endocrine Disrupting Compound by Granular Activated Carbon. 1. Adsorption Capacity and Kinetics. Environ. Sci. Technol. 43, 1467–1473. https://doi.org/10.1021/es801961y

Zuo, L., Ai, J., Fu, H., Chen, W., Zheng, S., Xu, Z., Zhu, D., 2016. Enhanced removal of sulfonamide antibiotics by KOH-activated anthracite coal: Batch and fixed-bed studies. Environ. Pollut. 211, 425–434. https://doi.org/10.1016/j.envpol.2015.12.064

Figure Captions

Figure 1. Breakthrough curves and fittings of the experimental data to the Yan model for the adsorption of CBZ onto PSA-PA at flow rates of 4.3 L d^{-1}, 8.6 L d^{-1} and 13 L d^{-1}, in a) distilled water and b) wastewater.

Figure 2. Breakthrough curves and fittings of the experimental data to the Yan model for the fixed-bed adsorption of CBZ, SMX and PAR onto PSA-PA at a flow rate of 4.3 L d^{-1} from a) single and b) ternary solutions in wastewater.

Figure 3. Breakthrough curves and fittings of the experimental data to the Yan model for the fixed-bed adsorption of CBZ from distilled water for 3 cycles of PSA-PA utilization: cycle 0 – virgin PSA-PA; cycle 1 – after first regeneration; and cycle 2 – after second regeneration.

Table 1. Efficiency and mass transfer parameters determined from the breakthrough curves corresponding to the fixed-bed adsorption of pharmaceuticals onto PSA-PA in distilled water and wastewater

	Q (L d^{-1})	mass of adsorbent (g)	$t_{10\%}$ (d)	V_b (L)	$q_{10\%}$ (mg g^{-1})	t_{total} (d)	q_{total} (mg g^{-1})	h_{MTZ} (cm)	EBCT (d)	U_r (g L^{-1})
					Distilled water (single solution)					
CBZ	4.3	3.55	2.92	12.61	**1.01**	17.58	**39.91**	2.49	0.0029	0.28
	8.6	3.61	0.83	7.17	0.79	8.72	31.66	2.49	0.0014	0.50
	13.0	3.56	0.21	2.72	0.20	4.00	19.95	2.53	0.0010	1.31
					Wastewater (single solution)					
	4.3	3.56	**0.33**	1.41	**0.14**	4.28	**6.65**	2.50	0.0029	2.52
CBZ	8.6	3.56	**0.10**	0.90	**0.07**	2.38	**7.00**	2.52	0.0014	3.96
	13.0	3.56	0.01	0.09	0.01	0.60	2.34	2.54	0.0010	39.18
SMX	4.3	3.56	0.10	0.45	0.03	1.46	2.23	2.52	0.0029	7.91
PAR	4.3	3.56	0.01	0.04	0.00	4.00	4.46	2.55	0.0029	82.29
					Wastewater (ternary solution)					
CBZ	4.3	3.56	**0.03**	0.14	0.01	3.17	5.58	2.55	0.0029	26.34
SMX	4.3	3.56	0.06	0.24	0.02	1.88	0.67	2.46	0.0029	14.80
PAR	4.3	3.56	0	0	0.00	4.21	8.57	2.55	0.0029	-
					Distilled water after regeneration					
CBZ – cycle 1	4.3	3.56	1.54	6.65	0.62	10.38	24.95	2.49	0.0029	0.53
CBZ – cycle 2	4.3	3.56	0.29	1.25	0.14	6.88	11.49	2.52	0.0029	2.82

Q - flow rate; $t_{10\%}$ - breakthrough time; V_b - volume treated at breakthrough; $q_{10\%}$ - mass of adsorbate adsorbed at breakthrough per gram of ads
t_{total} - total flow time; q_s – maximum mass of adsorbate adsorbed at saturation per gram of adsorbent; h_{MTZ} - height of the mass transfer zone; EB
empty bed contact time; U_r - usage rate; FBU - fraction bed utilization

Table 2. Fitting parameters of the Thomas, Yoon-Nelson and Yan models to the experimental data of the fixed-bed adsorption of CBZ onto PSA-PA.

Model	Parameters	CBZ in distilled water			CBZ in wastewater	
		Flow rate (L d^{-1})				
		4.3	*8.6*	*13.0*	*4.3*	*8.6*
Thomas	q_{Th} (mg g^{-1})	64.3 ± 1.2	52.1 ± 1.8	43.1 ± 1.7	15.5 ± 0.9	13.6 ±
	k_{Th} (L d^{-1} mg^{-1})	0.049 ± 0.002	0.094 ± 0.007	0.15 ± 0.01	0.14 ± 0.02	0.27 ±
	R^2	0.964	0.931	0.920	0.831	0.874
Yoon-Nelson	$t_{50\%}$ pred (d)	10.6 ± 0.2	4.3 ± 0.2	2.37 ± 0.09	2.6 ± 0.2	1.12 ±
	$t_{50\%}$ exp (d)	10.0	3.7	2.5	1.7	0.8
	k_{YN} (d^{-1})	0.25 ± 0.01	0.47 ± 0.04	0.76 ± 0.05	0.71 ± 0.08	1.4 ± (
	R^2	0.964	0.931	0.920	0.831	0.874
Yan	q_Y (mg g^{-1})	59.6 ± 0.6	45.9 ± 0.7	36.8 ± 1.2	12.5 ± 0.4	10.4 ±
	α^Y	1.91 ± 0.05	1.49 ± 0.04	1.01 ± 0.04	1.00 ± 0.04	0.98 ±
	R^2	0.993	0.993	0.978	0.980	0.992

q_{Th} - theoretical saturation adsorption capacity; k_{Th} - Thomas model rate constant; $t_{50\%}$ pred – time required for 50% of the adsorbate breakth
$t_{50\%}$ exp - experimental time required for 50% of the adsorbate breakthroughs; k_{YN} - Yoon-Nelson model rate constant; q_Y - amount of solute a

parameter; R^2 - coefficient of correlation

Table 3. Fitting parameters of the Thomas, Yoon-Nelson and Yan models to the experimental data of the fixed-bed adsorption of CBZ, SMX and PAR onto PSA-PA from single and ternary solutions in wastewater at a flow rate of 4.3 L d^{-1}.

Model	Parameters	Pharmaceutical				
		Single solution			**Ternary solution**	
		CBZ[a]	*SMX*	*PAR*	*CBZ*	*SMX*
Thomas	q_{Th} (mg g^{-1})	*15.5 ± 0.9*	5.3 ± 0.3	16.1 ± 1.1	6.9 ± 0.7	4.3 ± 0.5
	k_{Th} (L d^{-1} mg^{-1})	*0.14 ± 0.02*	0.45 ± 0.06	0.11 ± 0.01	0.30 ± 0.04	0.56 ± 0.08
	R^2	*0.831*	0.898	0.820	0.889	0.875
Yoon-Nelson	$t_{50\%}$ pred (d)	*2.6 ± 0.2*	0.86 ± 0.05	2.6 ± 0.2	1.1 ± 0.1	0.70 ± 0.07
	$t_{50\%}$ exp (d)	*1.7*	0.8	1.3	0.6	0.6
	k_{YN} (d^{-1})	*0.71 ± 0.08*	2.3 ± 0.3	0.54 ± 0.06	1.5 ± 0.2	2.8 ± 0.4
	R^2	*0.831*	0.898	0.820	0.889	0.875
Yan	q_Y (mg g^{-1})	*12.5 ± 0.4*	4.61 ± 0.08	13.5 ± 1.5	3.7 ± 0.2	2.67 ± 0.08
	α^Y	*1.00 ± 0.04*	1.15 ± 0.03	0.51 ± 0.04	0.83 ± 0.04	0.95 ± 0.03
	R^2	*0.980*	0.996	0.929	0.986	0.996

q_{Th} - theoretical saturation adsorption capacity; k_{Th} - Thomas model rate constant; $t_{50\%}$ pred - time required for 50% of the adsorbate breakthr
model; $t_{50\%}$ exp - experimental time required for 50% of the adsorbate breakthroughs; k_{YN} - Yoon-Nelson model rate constant; q_Y - amount of s
model parameter; R^2 - coefficient of correlation

[a]values from Table 2

Table 4. Textural parameters of PSA-PA used in the subsequent fixed-bed adsorption cycles: cycle 0 (virgin PSA-PA), cycle 1 (after first regeneration) and cycle 2 (after second regeneration) and of PSA-PA after use in the cycle 2.

	N_2 adsorption at −196 °C						
			Dubinin-Radushkevich (DR)			Dubinin-Astakhov (DA)	
	S_{BET} ($m^2 g^{-1}$)	V_p ($cm^3 g^{-1}$)	W_0 ($cm^3 g^{-1}$)	L (nm)	D (nm)	W_0 ($cm^3 g^{-1}$)	L (nm)
Cycle 0[a]	*671*	*0.37*	*0.27*	*1.44*	*1.11*	*0.28*	*1.58*
Cycle 1	617	0.35	0.25	1.34	1.12	0.27	1.62
Cycle 2	463	0.29	0.19	1.65	1.25	0.20	1.69
After use in cycle 2	391	0.24	0.16	-	1.25	0.17	1.77

V_p = total pore volume; W_0 = micropore volume; L = average micropore width; D = average pore diameter

[a]Values from Jaria et al. (2019)

Table 5. Fitting parameters of the Thomas, Yoon-Nelson and Yan models to the experimental data of the fixed-bed adsorption of CBZ onto PSA-PA from distilled water after regeneration stages 1 and 2, at a flow rate of 4.3 L d^{-1}.

Model	Parameters	Fixed-bed adsorption cycles		
		Cycle 0[a]	*Cycle 1*	*Cycle 2*
Thomas	q_{Th} (mg g^{-1})	64.3 ± 1.2	41.3 ± 0.5	20.62 ± 0.99
	k_{Th} (L d^{-1} mg^{-1})	0.049 ± 0.002	0.082 ± 0.003	0.103 ± 0.009
	R^2	0.964	0.979	0.902
Yoon-Nelson	$t_{50\%}$ pred (d)	10.6 ± 0.2	6.80 ± 0.08	3.4 ± 0.2
	$t_{50\%}$ exp (d)	10.0	6.7	2.7
	k_{YN} (d^{-1})	0.25 ± 0.01	0.41 ± 0.01	0.52 ± 0.04
	R^2	0.964	0.979	0.902

Yan	q_Y (mg g^{-1})	59.6 ± 0.6	38.8 ± 0.6	16.1 ± 0.5
	α^Y	1.91 ± 0.05	2.03 ± 0.09	1.11 ± 0.05
	R^2	0.993	0.981	0.984

q_{Th} - theoretical saturation adsorption capacity; k_{Th} - Thomas model rate constant; $t_{50\%}$ pred - time required for 50% of the adsorbate breakthroughs predicted by the model; $t_{50\%}$ exp - experimental time required for 50% of the adsorbate breakthroughs; k_{YN} - Yoon-Nelson model rate constant; q_Y - amount of solute adsorbed; α^Y - Yan model parameter; R^2 - coefficient of correlation

[a]values from Table 3

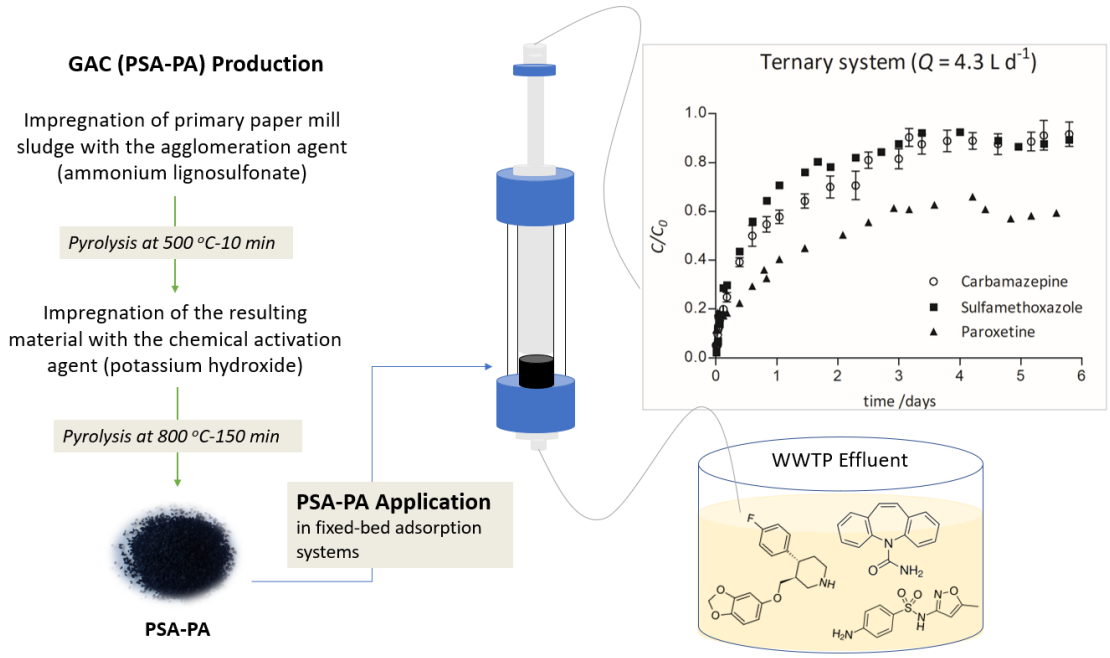

Graphical abstract

Highlights

1. An alternate granular activated carbon was used in the fixed-bed adsorption of drugs
2. Fixed-bed adsorption of 3 pharmaceuticals was tested in single and ternary systems
3. Flow rate influenced the adsorption of carbamazepine from distilled and wastewater
4. Bed capacity for the ternary system followed the order PAR > CBZ > SMX
5. Thermal regeneration of the carbon was evaluated for two serial adsorption cycles

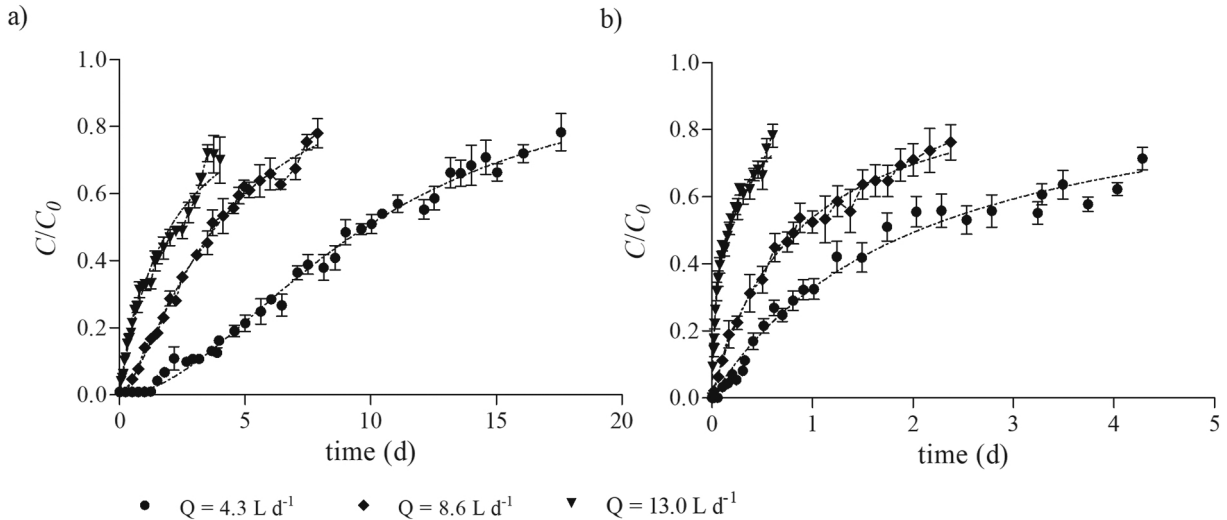

Figure 1

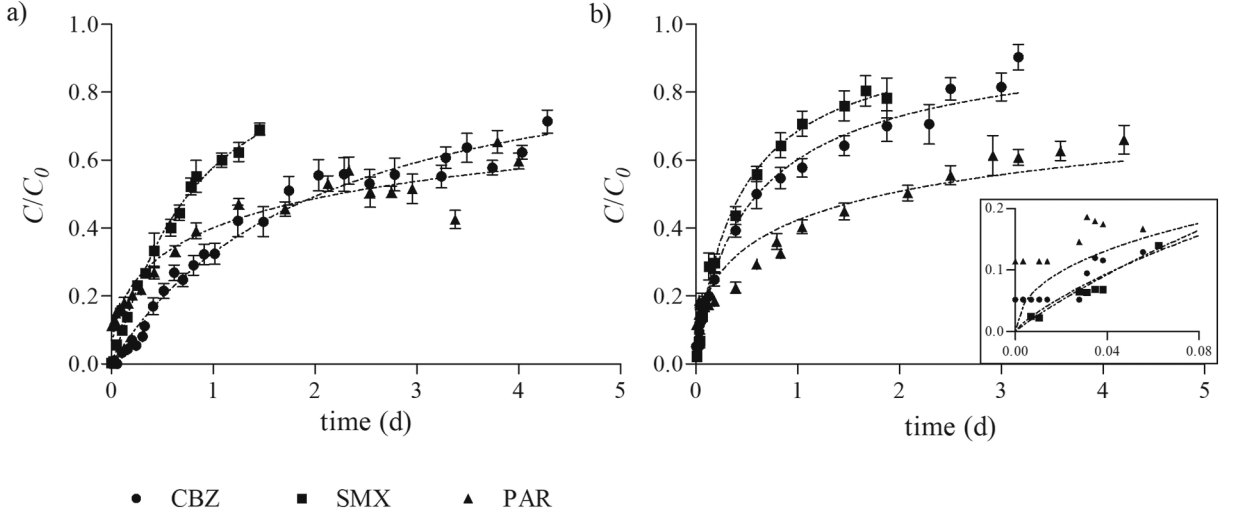

Figure 2

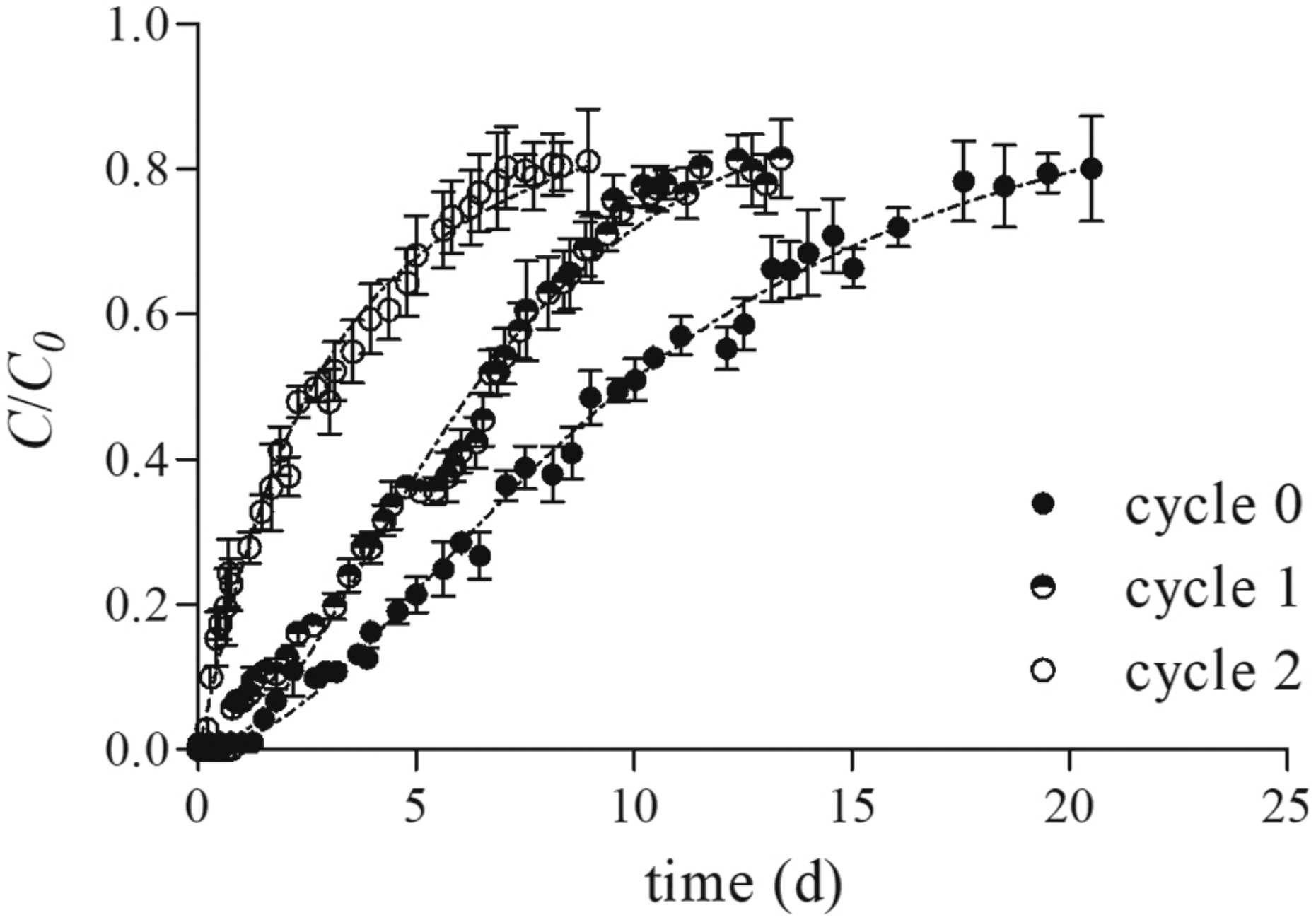

Figure 3